SCIENTIFIC REPORTS
nature research

OPEN

Porous materials of nitrogen doped graphene oxide@SnO_2 electrode for capable supercapacitor application

Received: 22 May 2019
Accepted: 16 August 2019
Published online: 02 September 2019

Sivalingam Ramesh[1], H. M. Yadav[2], Young-Jun Lee[3], Gwang-Wook Hong[3], A. Kathalingam[4], Arumugam Sivasamy[5], Hyun-Seok Kim[6], Heung Soo Kim[1] & Joo-Hyung Kim[3]

The porous materials of SnO_2@NGO composite was synthesized by thermal reduction process at 550 °C in presence ammonia and urea as catalyst. In this process, the higher electrostatic attraction between the SnO_2@NGO nanoparticles were anchored via thermal reduction reaction. These synthesized SnO_2@ NGO composites were confirmed by Raman, XRD, XPS, HR-TEM, and EDX results. The SnO_2 nanoparticles were anchored in the NGO composite in the controlled nanometer scale proved by FE-TEM and BET analysis. The SnO_2@NGO composite was used to study the electrochemical properties of CV, GCD, and EIS analysis for supercapacitor application. The electrochemical properties of SnO_2@ NGO exhibited the specific capacitance (~378 F/g at a current density of 4 A/g) and increasing the cycle stability up to 5000 cycles. Therefore, the electrochemical results of SnO_2@NGO composite could be promising for high-performance supercapacitor applications.

The nanotechnology of graphene-based materials are widely fabricated as active electrode for supercapacitor applications in presence of various strong electrolytes. In particular, the graphitic carbon electrodes are important role in the supercapacitor device applications[1–6]. Graphene is 2D carbon materials that contains high thermal conductivity, electrical conductivity, carrier mobility, and lateral quantum efficiencies. The carbon based materials are great interest because of the increasing the electronic capacity, mechanical properties, and superior chemical stability for photovoltaics, supercapacitors, and fuel cells applications[5,7–12]. The electrochemical performance of porous carbon material as electrical double layer capacitors (EDLC) is mainly depends on porosity, electrical conductivity, its dielectric constant, and various electrolytes. Based on the properties, the hybrid materials are classified into ultra-capacitor and conventional capacitors in the electrochemical reaction and its mechanism[13–17]. Recently, the N-doped graphene oxides (NGO) are widely used as electrode materials for supercapacitor, sensors and batteries studied in detail[18–20]. The NGO-metal oxides were synthesized to improve the electrochemical properties such as rate capability by using different catalyst[21,22]. Already the numerous research work reported on the NGO with metal oxides fabrication via CVD and thermal annealing process for supercapacitor and batteries applications. The various nanostructured metal oxides are fabricated in the electrochemical studies for increasing the specific capacitance and cyclic stability. In particular, the tin oxide (SnO_2) is an n-type semiconducting material and its excellent chemical properties allow to fabricate electrodes, which used as the candidate for supercapacitor applications[23,24]. The nanostructured SnO_2 is the most favorable metal oxides due to its increasing the capacitance, low cost, less poisonousness, and wide band gap ~3.6 eV. The various nanostructured SnO_2/

[1]Department of Mechanical, Robotics and Energy Engineering, Dongguk University-Seoul, Pil-dong, Jung-gu, 04620, Seoul, Republic of Korea. [2]Department of Energy and Materials Engineering, Dongguk University-Seoul, Pildong-ro 1 gil, Jung-gu, Seoul, 04620, Seoul, Republic of Korea. [3]Department of Mechanical Engineering, Inha University, Inha-ro 100, Nam-gu, Incheon, 402-751, Republic of Korea. [4]Millimeter-wave Innovation Technology (MINT) Research Center, Dongguk University-Seoul, Pil-dong, Jung-gu, 04620, Seoul, Republic of Korea. [5]Department of Chemical Engineering Area, Central Leather Research Institute (CLRI-CSIR), Adyar, Chennai, 600020, India. [6]Division of Electronics and Electrical Engineering, Dongguk University-Seoul, Pil-dong, Jung-gu, 04620, Seoul, Republic of Korea. Correspondence and requests for materials should be addressed to H.S.K. (email: heungsoo@dgu.edu) or J.-H.K. (email: joohyung.kim@inha.ac.kr)

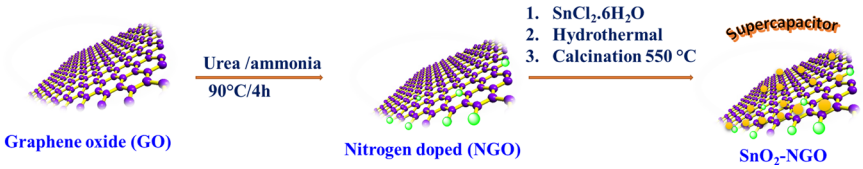

Figure 1. Schematic illustration of SnO_2@NGO synthesis via thermal reduction process.

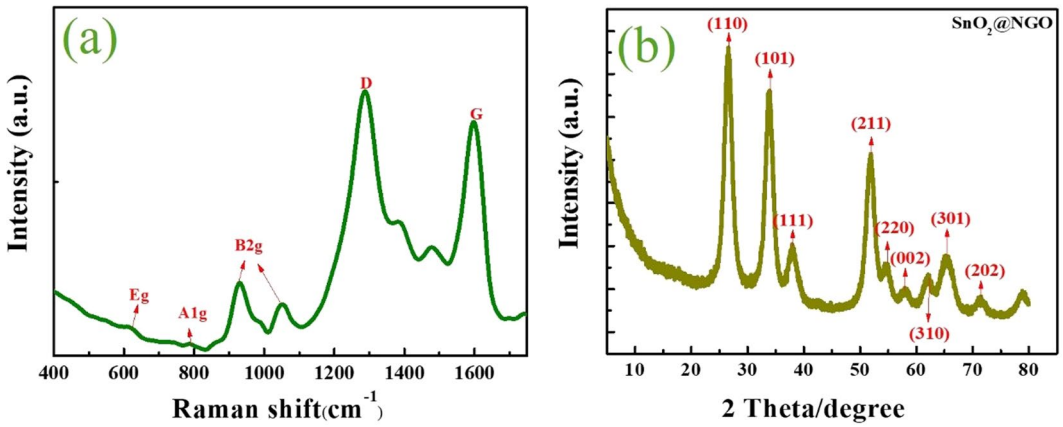

Figure 2. (**a**) Raman, and (**b**) XRD of SnO_2@NGO composite.

carbon composite was synthesized by hydrothermal process for electrochemical supercapacitor, sensors, and solar cells[25–29]. The SnO_2 and RuO_2 mixtures are used in the electrode materials for storage properties with an excellent cyclic stability[30]. The SnO_2/graphene composite reported the increasing electrochemical performance and cyclic stability via microwave synthesis[31]. The construction of Ni/SnO_2 composite shows an excellent capacitance and cyclic retention reported in the literature[32]. The hierarchical SnO_2 composite displays the specific capacitance of ~188 F/g with 2000 cycles[33]. In the present study, SnO_2@NGO composite was synthesized and it's electrochemical properties investigated by CV analysis. The SnO_2@NGO composite was analyzed by using Raman, XRD, XPS, BET, SEM, EDS, and HR-TEM analysis. Furthermore, the SnO_2@NGO composite was studied by CV, GCD, and EIS techniques with 6 M KOH electrolyte.

Results and Discussion

Structural and surface morphology of SnO_2@NGO. The schematic illustration of SnO_2@NGO synthesis via thermal reduction process is depicted in Fig. 1. The Raman spectral analysis used to study the carbon-based materials and its defect structure. Figure 2(a) represent the Raman results of graphene oxide (GO) and NGO obtained by a thermal reduction reaction. The properties of graphene materials are represented at 1,580 cm^{-1} to the E_{2g} peaks of sp^2 C atoms, and D band at 1,350 cm^{-1}, which was ascribed to the breathing modes of the A_{1g} symmetry[34]. These peaks provide the information of local defects and disorder behavior of NGO by Raman spectroscopy (Fig. 2a). The Raman peaks represented that the D band at 1358 cm^{-1} and G bands 1597 cm^{-1} in the NGO structure. Moreover, the D/G intensity of NGO decreased when comparted to GO composite. The intensity change is may be due to the reduction of the NGO materials by thermal reduction process in the sp^2 carbon structure. The peak position at lower wave numbers represent the different vibration modes of SnO_2 nanoparticles in the NGO composite[35,36].

The XRD studies of GO indicated the peak at about $2\theta = 10.80°$ with d -spacing 0.89 nm. The typical XRD peak of GO confirmed the well exfoliated carbon sheets in graphite structure has been reported previously[37–39]. The peak position at $2\theta = (9.84°$ and $19.7°)$, corresponds to the (002) and (100) planes of GO materials. This may be due to the thermal reduction of GO to graphitic crystal structure in presence of high temperature. In addition, the diffraction pure SnO_2 was studied in previous reports[40–43] and SnO_2@NGO diffraction peaks are represented in Fig. 2(b). The XRD of SnO_2@NGO composite at 26.57°, 33.87°, 37.86°, 52.26°, 54.93°, 57.87°, 62.15°, 65.33°, and 71.28° are clearly distinguishable and corresponding planes (110), (101), (111), (211), (220), (002), (310), (301) and (202), respectively. The structure of tetragonal confirmed the PDF file no: JCPDS 41–1445. Therefore, the SnO_2@NGO composite, which might be due to the exfoliation of NGO sheets at 550 °C by thermal reduction process.

Figure 3 represent the XPS peaks of SnO_2@NGO composite. The survey spectrum (Fig. 3d) indicates that C 1s (285), O 1s (532), and Sn3d (487) eV, which complete the effective adornment of SnO_2 nanoparticles onto the NGO surface. The Fig. 3c of Sn3d shows the main peaks of ($3d_{5/2}$) and $3d_{3/2}$ corresponds to the binding energies of 487.0 eV and 495.5 eV, respectively. The binding energy difference between $Sn3d_{5/2}$ and $Sn3d_{3/2}$ almost ~8.7 eV. These results confirmed the identical to the binding energies of SnO_2 and compared to the previous reports[44–46].

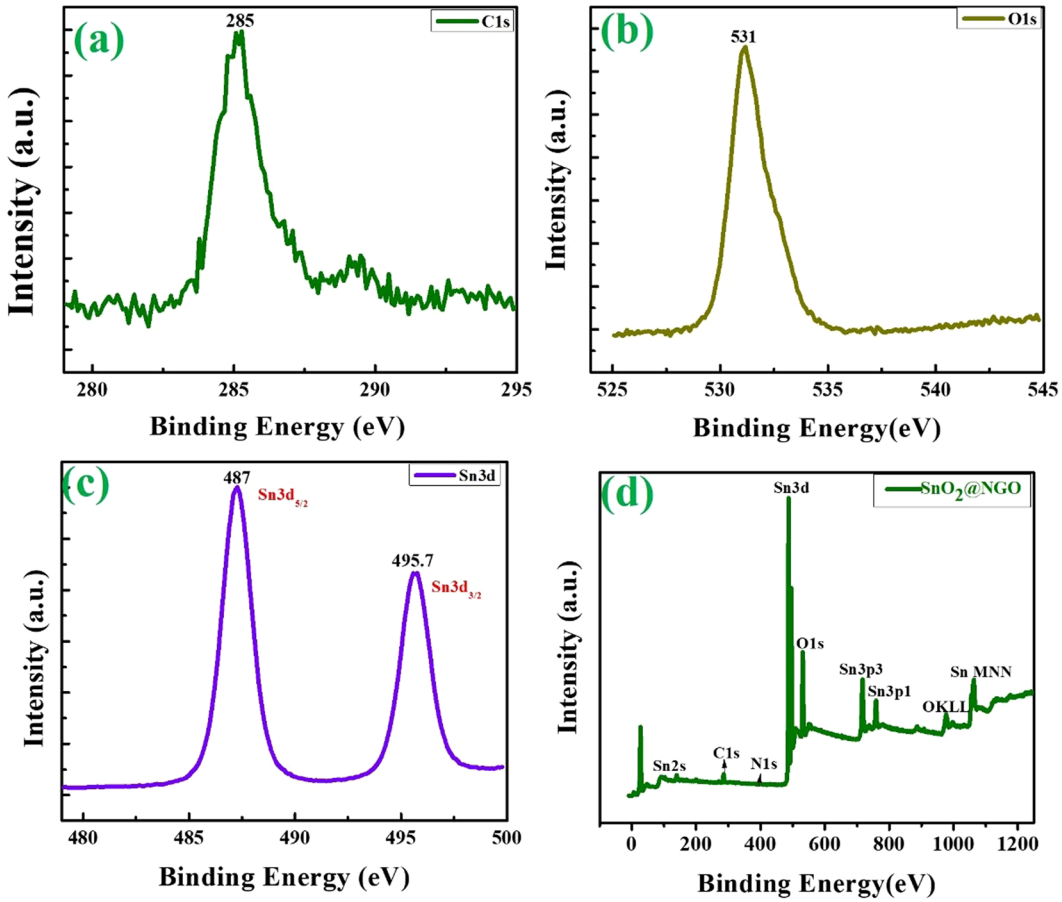

Figure 3. XPS results of (**a**) C 1s (**b**) O 1s (**c**) Sn 3d and (**d**) survey spectrum of SnO_2 @NGO composite.

Figures 4 and 5 represent morphological behaviors of SnO_2@NGO composite studied by FE-TEM analysis. The (Fig. 4a–c) morphology of shows that altered the magnifications of NGO composite. The nanocrystalline SnO_2 nanoparticles was decorated on the NGO and size of the particles in the range of ~10–20 nm (Fig. 4d). The high-resolution TEM of SnO_2@NGO composite (Fig. 4a–c) represent the distance of the SnO_2 nanoparticles are ~0.28 nm, matching to the (110) plane of SnO_2. The SAED image of the SnO_2@NGO (Fig. 4h) represent that the nanocrystalline behavior and this results consistent with XRD analysis of the composite. Figure 5 shows the different magnifications of SEM, SEM-EDS results confirms the C, O, N and Sn (Fig. 6) elements of the composite. In these results the N-doping level (32 wt %) on GO was achieved by simple hydrothermal method. The BET results are depicted in the Fig. 7. The surface area of the SnO_2@NGO composite of about ~180 m^2/g, pore volume of 0.27 cm^3/g, and pore area of ~130 m^2/g. The BJH analysis results are confirmed a mean pore size of the nanoparticles are ~(10–20) nm in the SnO_2@NGO composite.

Electrochemical measurements of SnO_2@NGO composite. The electrochemical results of GO, RGO, NGO and SnO_2 composite and its supercapacitor properties were reported in the previous studies[26,47–49]. The SnO_2@NGO composite was studied by cyclic voltammetric analysis results are shown in Fig. 8 and Table 1. The composite results indicate the ideal capacitive nature showing the rectangular profile owing to outstanding trend for supercapacitor. The trend of CV curves of composite electrodes, rectangular properties and corresponding increase of current than that of pristine SnO_2. These properties of composite shows the increasing the specific capacitance because of the combined influence from EDLC and pseudo capacitance of the composite. Figure 8a represent the CV results of SnO_2@NGO composite electrodes with the scanning rate from (10–100) mV s^{-1} in presence of 6 M KOH aqueous electrolyte. The electrochemical properties were studied the potentials range between (−0.2 and 0.8 V), it can be seen that the increasing the capacitance behaviors between the electrode and electrolyte. The scan rates increases, the current density also increases, because of the anodic and cathodic current change towards the reversible reaction. This fast redox or reversible reactions occurring between the electro-active material/electrolyte interfaces in presence 6 M KOH. Because of the CV represent a slight alteration with certain number of functional groups react in the NGO and SnO_2 nanoparticles. The specific capacitance of SnO_2@NGO electrodes are intended from the CV curves. The cyclic voltammetry results are shown Fig. 8a. In this CV experiments, the scan rate increased from 10 to 100 mV s^{-1} and also increases the electrochemical supercapacitor properties. The enhancement of electrochemical properties of the composite is mainly denoted to the more electroactive sites via EDLC and pseudo capacitance arises in the SnO_2@NGO composite. Further,

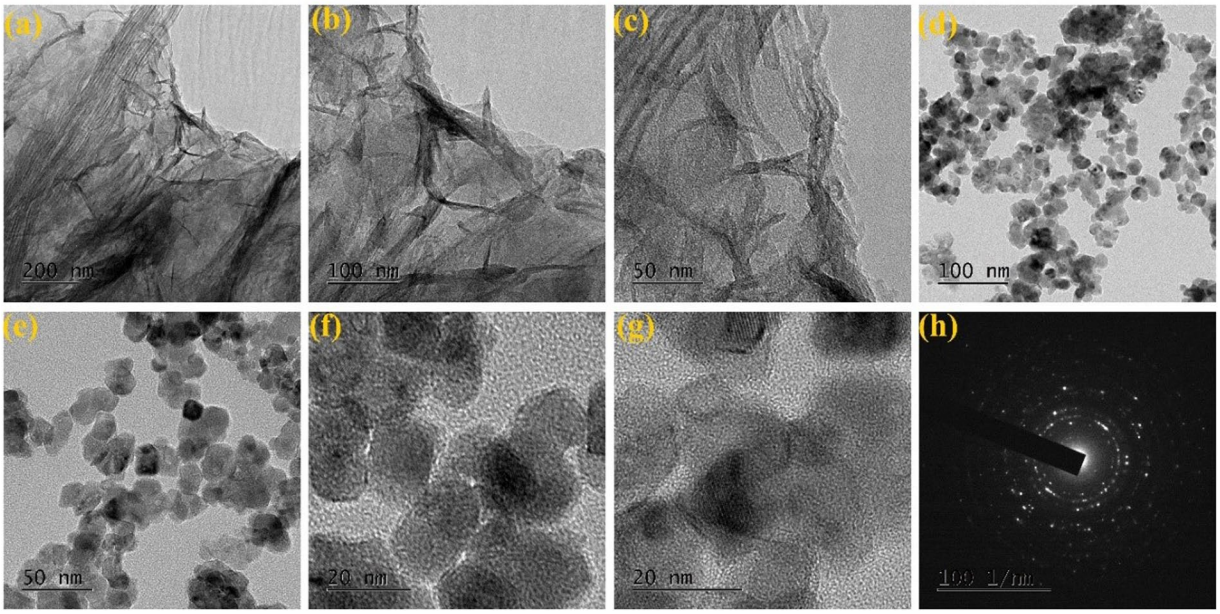

Figure 4. (**a**–**c**) TEM morphology of NGO materials, (**d**–**g**) HR- images of SnO_2@NGO composite and (**h**) SAED pattern of composite.

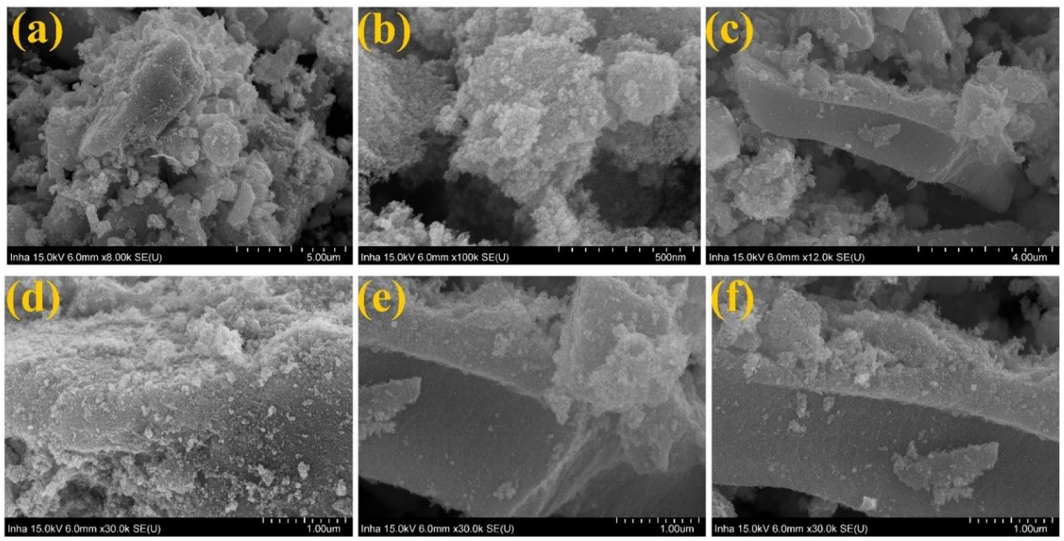

Figure 5. (**a**–**f**) SEM-Morphology of SnO_2@NGO composite.

the SnO_2 nanoparticles at the NGO matrix successfully decorated and low internal resistance with high electrical conductivity of the composite for electrochemical reversible reaction[26,47–49].

Furthermore, the SnO_2@NGO composite for charge-discharge test from the GCD curves represented in Fig. 8(b). The GCD curves of composite electrodes are increases the current density of 4, 8.5 and 12.6 A/g by using 6 M KOH solution. The GCD results evidently designates the triangular shape of the composite materials and the contribution of EDLC and pseudo capacitance properties from CV analysis. The composite electrodes are confirmed the higher discharge time than that of pristine SnO_2 composite represent the increasing specific capacitance with stronger electrolytes[26,47–49].

The specific capacitance values are ~378 F/g, 345 F/g, and 230 F/g at the current density of 4, 8.5, and 12.6 A/g, respectively. The Fig. (8c,d) represent the cyclic retention and corresponds to the current density (*vs*) its specific capacitance values. The trend of the specific capacitance values was decreased, as the current density increased 4, 8.5, and 12.6 A/g. Because of the diffusion of the electrolyte ions, depends on the morphology, surface of the materials and concentration of the SnO_2 and NGO components. The electrochemical properties of the SnO_2@NGO nanoparticles was compared to the previous reports for supercapacitor applications[50–52].

In addition, the SnO_2@NGO composite, energy density and power density results are shown in Fig. 8(e,f). The cyclic stability is the important property of the electrode for practical applications in the supercapacitors.

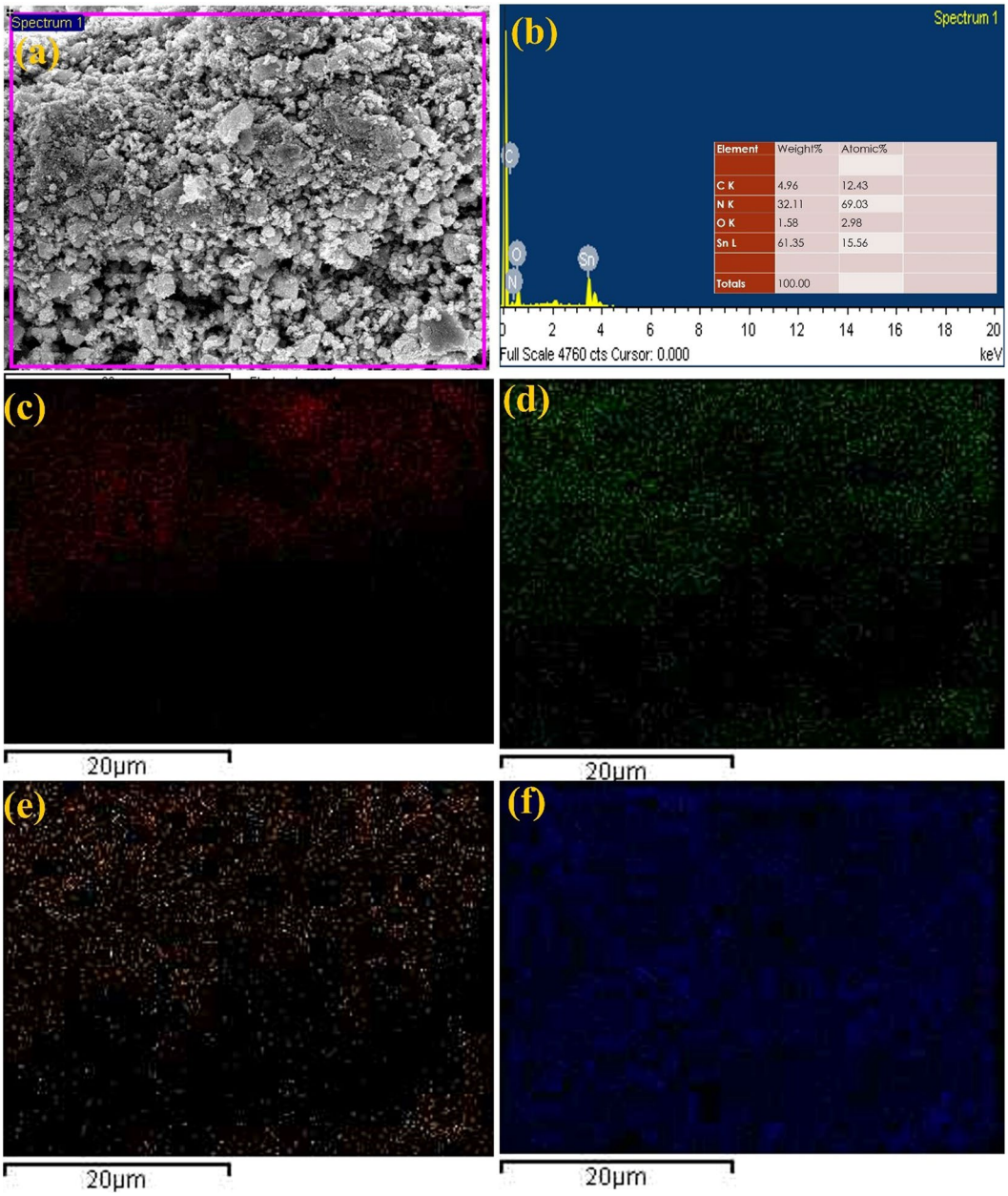

Figure 6. (**a**–**b**) SEM-EDS and (**c**) C 1s (**d**) O 1s (**e**) N 1s and (**f**) Sn 3d morphology of SnO_2@NGO composite.

Figure 8(c) shows the GCD analysis at a current density of 4 A/g for 5,000 cycles. After 2,000 cycles, the composite electrode maintained 89% of its original performance, which signifies of electroactive material has better cyclic stability[49,53] and reversibility of the GCD process.

Furthermore, the EIS results were estimated at open circuit potential by relating the various ac voltages in the frequency range from 0.1 Hz to 100 kHz. Figure 8(d) represent the EIS result of Nyquist plots for SnO_2@NGO composite, which is indicate that the real and imaginary parts of EIS results, respectively. First, the smaller semi-circular loop at higher frequencies is attributed to the Faradaic reactions in presence of the 6 M KOH electrolyte. The lower frequency region of the EIS increases due to the capacitive nature of SnO_2@NGO composite. The phase angle of EIS of composite electrode was perceived to be higher than 45° and low frequencies demonstrating the electrochemical capacitive nature of the composite materials. In this regard, the charge transfer resistance (Rct) of the NGO and composite electrodes are ~36 and 38, respectively. In this lower value of Rct represent the stable electrochemical performance. The low-frequency region of the impedance analysis results are called Warburg resistance of diffusion behavior in presence of 6 M KOH with in the electrodes. The vertical slope of Warburg curves specifies the rapid development of an electric double-layer in the composite because of quick ion diffusion in presence of 6 M KOH electrolyte for supercapacitor applications[49,54].

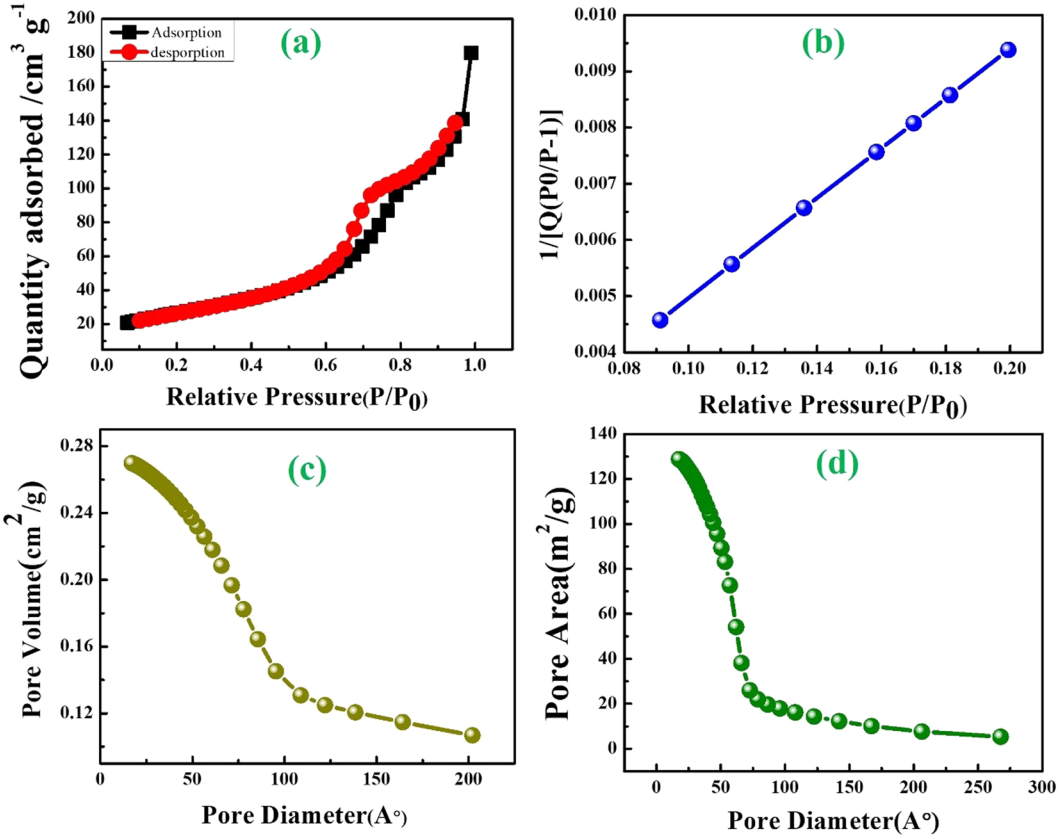

Figure 7. BET results of (**a**–**d**) SnO_2@NGO composite.

Conclusions

The porous material of SnO_2@NGO composite synthesized by thermal reduction process and studied their electrochemical characteristics towards high-performance supercapacitors. The Raman, X-ray diffraction, and photoelectron spectroscopy analysis reveals the successful formation of SnO_2@NGO composite. The specific capacitance of the SnO_2@NGO composite displayed the capacitance ~378 F/g at a current density of 4 A/g in the 6 M KOH solution. Moreover, the composite electrode exhibited an excellent cycling stability at 4 A/g. The composite electrode maintained 89% of its original performance after 5000 cycles in presence of 6 M KOH electrolyte, there by representing the plausible applicability for energy storage applications.

Materials and Methods

Materials. The graphene oxide from graphite flakes, sulfuric acid (H_2SO_4,), phosphoric acid (H_3PO_4), potassium permanganate ($KMnO_4$), potassium hydroxide (KOH), hydrogen peroxide (H_2O_2, 30%) in this experiment. The tin (IV) chloride pentahydrate ($SnCl_4.5H_2O$, 98%), ammonia solution (NH_3, 30%), N-methyl-2-pyrrolidone and polytetrafluorethylene (PTFE) were chemicals received from Sigma-Aldrich, South Korea.

Graphene oxide synthesis (GO). The graphene oxide (GO) materials were developed by Hummer's technique in the previous reports[27–29]. The graphite (5 g), H_2SO_4 (400 mL), H_3PO_4 (50 mL), and $KMnO_4$ (18 g) were mixed in the three-neck flask using a magnetic stirrer at 40 °C and continually stirred for 48 h to achieve the complete conversion from graphite. After that, the reaction mixture was changes from dark purple to greenish brown color and the calculate amount 20 mL of H_2O_2 was added to complete the conversion of GO. The GO was purified by using 1 M of HCl or ethanol and then purified the oven at 80 °C for 12 h.

N-Doped graphene oxide synthesis (NGO). The calculated amount of 0.5 g of GO was distributed in the 300 mL of distilled water followed by ultra-sonication and the solution becomes the brownish GO suspension. The GO suspension and required amount of 20 mL of excess of water is added and stirred for 4 h and filtered/dried in the vacuum oven at 90 °C for 4 h. Then the calculated amount of 1 g of urea and ammonia and excess of 20 mL of ammonia was added and continuously stirred at 90 °C for 12 h. Finally, the GO product was dried in the oven at 200 °C for 12 h, and purified by using ethanol solvent.

SnO_2@NGO composite synthesis. Briefly, 0.2 g of GO was distributed in 150 mL of water and sonication for 1 h to become the homogeneous solution. Then the calculated amount of 1.2 g of stannous chloride, 25% of 10 mL ammonia solution was added to the GO solution to maintain the basic medium. Afterwards, the reaction GO solution was refluxed at 200 °C for 8 h by using three neck flask with condenser. Then, the reaction becomes

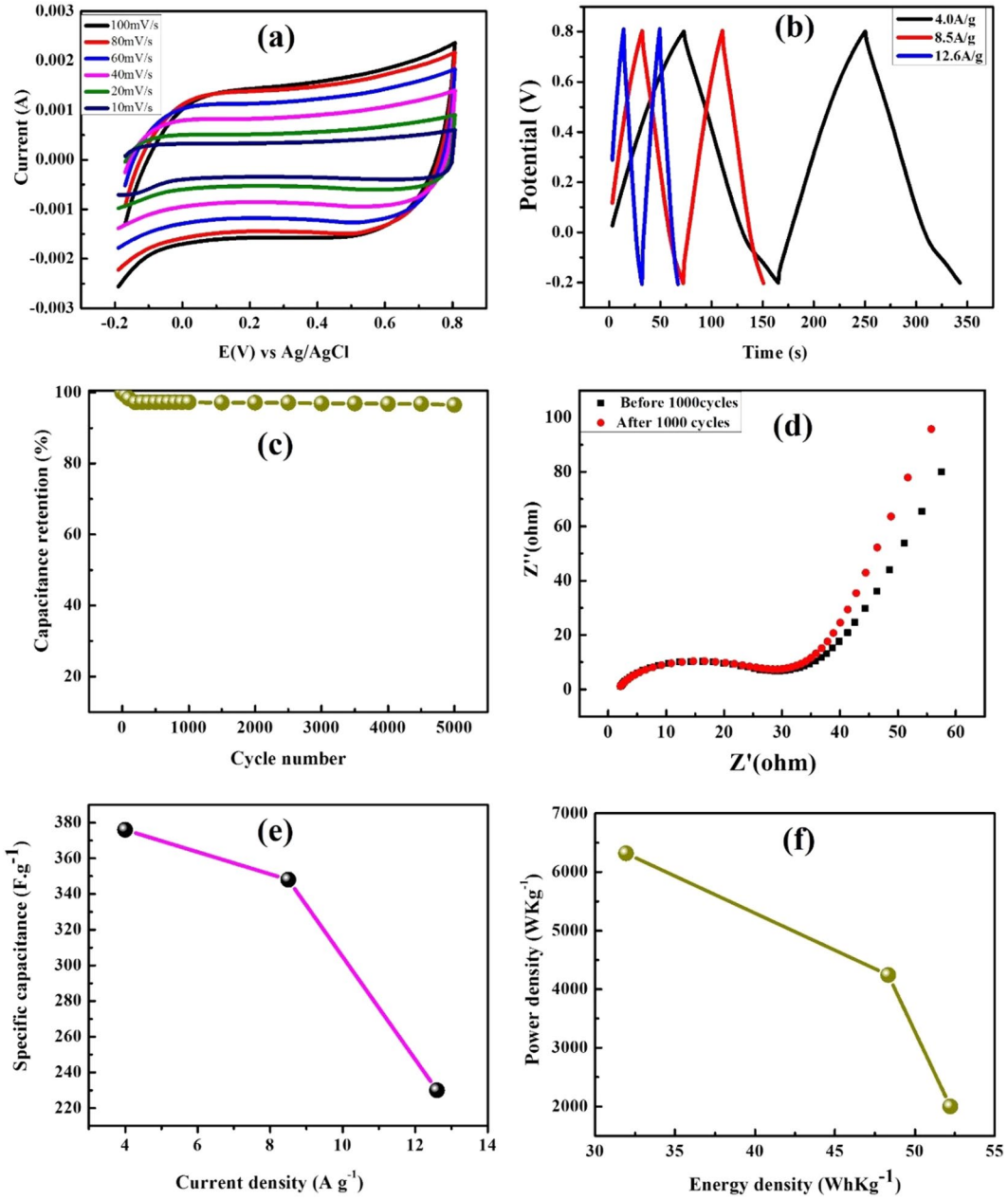

Figure 8. (**a**) CVs of the SnO_2@NGO composite electrodes at various scan rates of (10–100) mV s^{-1} in 6 M KOH. (**b**) Charge/discharge profiles of the composite electrode at different current densities (4, 8.5, and 12.6) A/g. (**c**) Variation of specific capacitance as a function of cyclic number at a current density of 4.0 A/g, (**d**) EIS, and (**e**) the effect of Energy density *vs*. Power density.

changed to black color product of SnO_2@NGO and dried in the vacuum oven at 180 °C for 12 h. Further, the SnO_2@NGO sample was calcination at 550 °C for 8 h and collected the product for further characterization.

Preparation of electrochemical analysis. The CV experiment was studied in the regular three-electrode system connected through Autolab PGSTAT302N (Metrohm, Netherlands). The SnO_2@NGO composite (working electrode), carbon black, and PVDF in the stoichiometric of 75: 15: 10 and dispersed in the n-methyl 2-pyrrolidone. The resulted black paste was then covered onto a nickel wire collector and dried at 110 °C for 12 h. The mass loading of the SnO_2@NGO composite is around 1.5 mg cm^{-2}. In this experiment, platinum wire (counter electrode) and Ag/AgCl (reference electrode) were fabricated in the CV analysis. The synthesized SnO_2@NGO composite and its electrochemical properties were determined by cyclic voltammetry analysis. The CV curves were documented at various scan rates (10, 20, 40, 60, 80, and 100) mV s^{-1} in a potential range of (−0.2 to 0.8) V. The GCD curves were acquired at various current densities (4, 8.5 and 12.6) A/g and EIS results in the frequency range of (0.1 Hz to 100 kHz). The capacitance of SnO_2@NGO composite was designed from the CV Eq. (1), and GCD curves Eq. (2) were shown in the previous reports[30–33].

Electrode material	Preparation method	Capacitance (F/g)	Cyclic stability	Ref.
SnO_2@C nanoparticles	Calcination process at (500–700) °C	37.8 F/g at 5 mV/s	NA	54
$SO4^{2-}/SnO_2$ nanocomposite	Alkaline hydrolysis	51.95 F/g at 5 mV/s	7.5% loss after 2,000 cycles	55
Hydrous SnO_2 Thin films composite	Chemical Synthesis of Thin film	25 F/g at 5 mV/s	NA	56
MWCNT/SnO_2 composite	Decoration by sonochemical process	133.33 F/g at 0.5 mV/s	10% loss after 500 cycles	57
GO/SnO_2	Spray pyrolysis	61.7 F/g at 1 A/g	1% loss after 106 cycles	52
SnO_2/Graphene	Microwave assisted one-pot reaction	99.7 F/g at 5 mV/s1	NA	48
GNs/SnO_2–MWCNTs	Chemical method followed by calcination	224 F/g at 10 mA	8% loss after 6000 cycles	58
RGO/SnO_2 composite	Microwave assisted deposition	348 F/g at 50 m A g^{-1}	2% loss after 1,000 cycles	59
SnO_2@NGO composite	**Thermal reduction process**	**378 F/g at 4 A/g**	**11% loss after 5,000 cycles**	**This work**

Table 1. Parameters for the supercapacitor of SnO_2 and SnO_2@NGO electrodes reported in the literature. NA-Not available.

Materials characterization. Raman studies were analyzed in the range (100 to 4000 cm^{-1}) by using RM200 confocal Raman spectroscopy. The composite was studied the wide-angle XRD analysis documented by Rigaku Rotaflex (RU-200B) diffractometry in presence Cu Kα radiation. The morphological properties of SnO_2@NGO were analyzed by using FE-SEM-4800, and JEM-2010F FE-TEM, Hitachi Japan. The SnO_2@NGO composite was examined by X-ray photoelectron spectroscopy by (Thermal Fisher Scientific, USA) with Kα radiation.

References

1. Simon, P. & Gogotsi, Y. Materials for electrochemical capacitors. *Nat. Mater.* **7**, 845–854 (2008).
2. Miller, J. R. & Simon, P. Materials science: Electrochemical capacitors for energy management. *Science*, https://doi.org/10.1126/science.1158736 (2008).
3. Zhang, Y. *et al.* Growth of 3D SnO_2 nanosheets on carbon cloth as a binder-free electrode for supercapacitors. *J. Mater. Chem. A*, https://doi.org/10.1039/c5ta02479j (2015).
4. Dhole, I. A., Navale, Y. H., Pawar, C. S., Navale, S. T. & Patil, V. B. Physicochemical and supercapacitive properties of electroplated nickel oxide electrode: effect of solution molarity. *J. Mater. Sci. Mater. Electron.*, https://doi.org/10.1007/s10854-018-8537-y (2018).
5. Min, J. *et al.* Facile synthesis of porous iron oxide/graphene hybrid nanocomposites and potential application in electrochemical energy storage. *New J. Chem.* **41**, 13553–13559 (2017).
6. Zhu, S. *et al.* Low-Charge-Carrier-Scattering Three-Dimensional α-MnO_2/β-MnO_2 Networks for Ultra-High-Rate Asymmetrical Supercapacitors. *ACS Appl. Energy Mater.* **2**, 1051–1059 (2019).
7. Maile, N. C. *et al.* Facial growth of $Co(OH)_2$ nanoflakes on stainless steel for supercapacitors: effect of deposition potential. *J. Mater. Sci. Mater. Electron.* **30**, 5555–5566 (2019).
8. Ramesh, S. *et al.* $Ni(OH)_2$-decorated nitrogen doped MWCNT nanosheets as an efficient electrode for high performance supercapacitors. *Sci. Rep.* **9**, 6034 (2019).
9. Ramesh, S., Haldorai, Y., Kim, H. S. & Kim, J.-H. A nanocrystalline Co_3O_4 @polypyrrole/MWCNT hybrid nanocomposite for high performance electrochemical supercapacitors. *RSC Adv.* **7**, 36833–36843 (2017).
10. Bhunia, K., Khilari, S. & Pradhan, D. Trimetallic PtAuNi alloy nanoparticles as an efficient electrocatalyst for the methanol electrooxidation reaction. *Dalt. Trans.* **46**, 15558–15566 (2017).
11. Salgado, S., Pu, L. & Maheshwari, V. Targeting Chemical Morphology of Graphene Oxide for Self-Assembly and Subsequent Templating of Nanoparticles: A Composite Approaching Capacitance Limits in Graphene. *J. Phys. Chem. C* **116**, 12124–12130 (2012).
12. Zhu, S. J., Zhang, J., Ma, J. J., Zhang, Y. X. & Yao, K. X. Rational design of coaxial mesoporous birnessite manganese dioxide/amorphous-carbon nanotubes arrays for advanced asymmetric supercapacitors. *J. Power Sources* **278**, 555–561 (2015).
13. Lozano-Castelló, D. *et al.* Influence of pore structure and surface chemistry on electric double layer capacitance in non-aqueous electrolyte. *Carbon N. Y.* **41**, 1765–1775 (2003).
14. Gupta, V. & Miura, N. Polyaniline/single-wall carbon nanotube (PANI/SWCNT) composites for high performance supercapacitors. *Electrochim. Acta* **52**, 1721–1726 (2006).
15. Wang, W., Hao, Q., Lei, W., Xia, X. & Wang, X. Graphene/SnO_2/polypyrrole ternary nanocomposites as supercapacitor electrode materials. *RSC Adv.* **2**, 10268 (2012).
16. Xu, J., Wang, K., Zu, S.-Z., Han, B.-H. & Wei, Z. Hierarchical Nanocomposites of Polyaniline Nanowire Arrays on Graphene Oxide Sheets with Synergistic Effect for Energy Storage. *ACS Nano* **4**, 5019–5026 (2010).
17. Yu, G. *et al.* Enhancing the Supercapacitor Performance of Graphene/MnO_2 Nanostructured Electrodes by Conductive Wrapping. *Nano Lett.* **11**, 4438–4442 (2011).
18. Ding, S., Luan, D., Boey, F. Y. C., Chen, J. S. & Lou, X. W. (David). SnO_2 nanosheets grown on graphene sheets with enhanced lithium storage properties. *Chem. Commun.* **47**, 7155 (2011).
19. Ning, G. *et al.* Three-dimensional hybrid materials of fish scale-like polyaniline nanosheet arrays on graphene oxide and carbon nanotube for high-performance ultracapacitors. *Carbon N. Y.* **54**, 241–248 (2013).

20. Zhao, L. *et al*. Nitrogen-Containing Hydrothermal Carbons with Superior Performance in Supercapacitors. *Adv. Mater.* **22**, 5202–5206 (2010).
21. Zhu, S. J. *et al*. Rational design of octahedron and nanowire CeO_2@MnO_2 core–shell heterostructures with outstanding rate capability for asymmetric supercapacitors. *Chem. Commun.* **51**, 14840–14843 (2015).
22. Zhu, S. *et al*. Structural Directed Growth of Ultrathin Parallel Birnessite on β-MnO_2 for High-Performance Asymmetric Supercapacitors. *ACS Nano* **12**, 1033–1042 (2018).
23. Xu, C., Sun, J. & Gao, L. Controllable synthesis of monodisperse ultrathin SnO_2 nanorods on nitrogen-doped graphene and its ultrahigh lithium storage properties. *Nanoscale* **4**, 5425 (2012).
24. Xu, C., Sun, J. & Gao, L. Direct growth of monodisperse SnO_2 nanorods on graphene as high capacity anode materials for lithium ion batteries. *J. Mater. Chem.* **22**, 975–979 (2012).
25. Yin, X. M. *et al*. One-Step Synthesis of Hierarchical SnO_2 Hollow Nanostructures via Self-Assembly for High Power Lithium Ion Batteries. *J. Phys. Chem. C* **114**, 8084–8088 (2010).
26. Li, F. *et al*. One-step synthesis of graphene/SnO_2 nanocomposites and its application in electrochemical supercapacitors. *Nanotechnology* **20**, 455602 (2009).
27. Pusawale, S. N., Deshmukh, P. R. & Lokhande, C. D. Chemical synthesis of nanocrystalline SnO_2 thin films for supercapacitor application. *Appl. Surf. Sci.* **257**, 9498–9502 (2011).
28. Sun, L. *et al*. Nitrogen-doped graphene with high nitrogen level via a one-step hydrothermal reaction of graphene oxide with urea for superior capacitive energy storage. *RSC Adv.* **2**, 4498 (2012).
29. Ramesh, S., Kim, H. S., Haldorai, Y., Han, Y.-K. & Kim, J.-H. Fabrication of nanostructured MnO_2/carbon nanotube composite from 3D precursor complex for high-performance supercapacitor. *Mater. Lett.* **196**, 132–136 (2017).
30. Duraivel, M. *et al*. Superior one-pot synthesis of a doped graphene oxide electrode for a high power density supercapacitor. *New J. Chem.* **42**, 11093–11101 (2018).
31. Selvan, R. K., Perelshtein, I., Perkas, N. & Gedanken, A. Synthesis of Hexagonal-Shaped SnO_2 Nanocrystals and SnO_2@C Nanocomposites for Electrochemical Redox Supercapacitors, https://doi.org/10.1021/JP076995Q (2008).
32. Chen, Y.-J., Zhu, C.-L., Xue, X.-Y., Shi, X.-L. & Cao, M.-S. High capacity and excellent cycling stability of single-walled carbon nanotube/SnO_2 core-shell structures as Li-insertion materials. *Appl. Phys. Lett.* **92**, 223101 (2008).
33. Xia, H., Wang, Y., Lin, J. & Lu, L. Hydrothermal synthesis of MnO_2/CNT nanocomposite with a CNT core/porous MnO_2 sheath hierarchy architecture for supercapacitors. *Nanoscale Res. Lett.* **6**, 595 (2011).
34. Saravanakumar, B., Purushothaman, K. K. & Muralidharan, G. Interconnected V_2O_5 Nanoporous Network for High-Performance Supercapacitors. *ACS Appl. Mater. Interfaces* **4**, 4484–4490 (2012).
35. Zhao, B. *et al*. Bivalent tin ion assisted reduction for preparing graphene/SnO_2 composite with good cyclic performance and lithium storage capacity. *Electrochim. Acta* **56**, 7340–7346 (2011).
36. Wang, S., Jiang, S. P. & Wang, X. Microwave-assisted one-pot synthesis of metal/metal oxide nanoparticles on graphene and their electrochemical applications. *Electrochim. Acta* **56**, 3338–3344 (2011).
37. Ramesh, S., Kathalingam, A., Karuppasamy, K., Kim, H.-S. & Kim, H. S. Nanostructured CuO/Co_2O_4@ nitrogen doped MWCNT hybrid composite electrode for high-performance supercapacitors. *Compos. Part B Eng.* **166**, 74–85 (2019).
38. Winter, M. & Brodd, R. J. What Are Batteries, Fuel Cells, and Supercapacitors?, https://doi.org/10.1021/CR020730K (2004).
39. Augustyn, V., Simon, P. & Dunn, B. Pseudocapacitive oxide materials for high-rate electrochemical energy storage. *Energy Environ. Sci.* **7**, 1597 (2014).
40. Hwang, S.-W. & Hyun, S.-H. Synthesis and characterization of tin oxide/carbon aerogel composite electrodes for electrochemical supercapacitors. *J. Power Sources* **172**, 451–459 (2007).
41. Zhang, L. L., Zhou, R. & Zhao, X. S. Graphene-based materials as supercapacitor electrodes. *J. Mater. Chem.* **20**, 5983 (2010).
42. Lei, Z., Zhang, J. & Zhao, X. S. Ultrathin MnO_2 nanofibers grown on graphitic carbon spheres as high-performance asymmetric supercapacitor electrodes. *J. Mater. Chem.* **22**, 153–160 (2012).
43. Algharaibeh, Z., Liu, X. & Pickup, P. G. An asymmetric anthraquinone-modified carbon/ruthenium oxide supercapacitor. *J. Power Sources* **187**, 640–643 (2009).
44. Yan, X., Tai, Z., Chen, J. & Xue, Q. Fabrication of carbon nanofiber–polyaniline composite flexible paper for supercapacitor. *Nanoscale* **3**, 212–216 (2011).
45. Liu, Y. *et al*. Enhanced electrochemical performance of hybrid SnO_2@MO_x (M = Ni, Co, Mn) core–shell nanostructures grown on flexible carbon fibers as the supercapacitor electrode materials. *J. Mater. Chem. A* **3**, 3676–3682 (2015).
46. Sun, J. *et al*. 3D core/shell hierarchies of MnOOH ultrathin nanosheets grown on NiO nanosheet arrays for high-performance supercapacitors. *Nano Energy* **4**, 56–64 (2014).
47. Xia, X. *et al*. Self-supported hydrothermal synthesized hollow Co_3O_4 nanowire arrays with high supercapacitor capacitance. *J. Mater. Chem.* **21**, 9319 (2011).
48. Lim, S. P., Huang, N. M. & Lim, H. N. Solvothermal synthesis of SnO_2/graphene nanocomposites for supercapacitor application. *Ceram. Int.* **39**, 6647–6655 (2013).
49. Zhang, M. *et al*. Fast synthesis of SnO_2/graphene composites by reducing graphene oxide with stannous ions. *J. Mater. Chem.* **21**, 1673–1676 (2011).
50. He, C. *et al*. Mosaic-Structured SnO_2@C Porous Microspheres for High-Performance Supercapacitor Electrode Materials. *Electrochim. Acta* **142**, 157–166 (2014).
51. Wang, R., Xu, C., Sun, J., Gao, L. & Yao, H. Solvothermal-Induced 3D Macroscopic SnO_2/Nitrogen-Doped Graphene Aerogels for High Capacity and Long-Life Lithium Storage. *ACS Appl. Mater. Interfaces* **6**, 3427–3436 (2014).
52. Lu, T. *et al*. Electrochemical behaviors of graphene–ZnO and graphene–SnO_2 composite films for supercapacitors. *Electrochim. Acta* **55**, 4170–4173 (2010).
53. Wang, Y., Lee, J. Y. & Zeng, H. C. Polycrystalline SnO_2 Nanotubes Prepared via Infiltration Casting of Nanocrystallites and Their Electrochemical Application, https://doi.org/10.1021/CM050724F (2005).
54. Cui, H., Liu, Y., Ren, W., Wang, M. & Zhao, Y. Large scale synthesis of highly crystallized SnO_2 quantum dots at room temperature and their high electrochemical performance. *Nanotechnology* **24**, 345602 (2013).
55. Gao, Y. *et al*. $SO4^{2-}$/SnO_2 as a new electrode for electrochemical supercapacitors. *Ceram. Int.* **40**, 8925–8929 (2014).
56. Pusawale, S. N., Deshmukh, P. R. & Lokhande, C. D. Chemical synthesis and characterization of hydrous tin oxide (SnO_2:H_2O) thin films. *Bull. Mater. Sci.* **34**, 1179–1183 (2011).
57. Vinoth, V. *et al*. SnO_2-decorated multiwalled carbon nanotubes and Vulcan carbon through a sonochemical approach for supercapacitor applications. *Ultrason. Sonochem.* **29**, 205–212 (2016).
58. Rakhi, R. B. & Alshareef, H. N. Enhancement of the energy storage properties of supercapacitors using graphene nanosheets dispersed with metal oxide-loaded carbon nanotubes. *J. Power Sources* **196**, 8858–8865 (2011).
59. Hsieh, C.-T., Lee, W.-Y., Lee, C.-E. & Teng, H. Electrochemical Capacitors Fabricated with Tin Oxide/Graphene Oxide Nanocomposites. *J. Phys. Chem. C* **118**, 15146–15153 (2014).

Acknowledgements

This research programme fully supported by the Basic Science Research Program through the National Research Foundation of Korea (NRF-2017R1D1A1B03028368, NRF-2017M3A9E2063256), funded by the Ministry and Institute for Information & communications Technology Promotion (IITP) grant funded by the Korea Government (MSIP) (No. R7520160005000 1002) and also supported under the frame work of 2017 International and Cooperation Programmed by National Research Foundation of Korea (Grant No. 2017K1A4A3013662).

Author Contributions

S.R. and H.S.K. design the project and the experiments for supercapacitor applications. S.R. carried out the experiments of SnO_2@NGO composite. All authors S.R., H.M.Y., Y.J.L., G.W.H., A.K., A.S., H.-S.K., H.S.K. and J.-H.K. involved in the characterization of the SnO_2@NGO composite and the discussions prominent up to the writing of the manuscript.

Additional Information

Competing Interests: The authors declare no competing interests.

Publisher's note: Springer Nature remains neutral with regard to jurisdictional claims in published maps and institutional affiliations.